Environment Canada
Water Science and Technology Directorate

Direction générale des sciences et de la technologie, eau
Environnement Canada

Measurement of the Hydraulic Properties of Low-Permeability Rock

By:

K. Novakowski & G. Bickerton

NWRI Contribution # 96-87

96-87

MEASUREMENT OF THE HYDRAULIC PROPERTIES OF LOW-PERMEABILITY ROCK

BY
KENTNER S. NOVAKOWSKI
AND
GREGORY S. BICKERTON

NATIONAL WATER RESEARCH INSTITUTE
867 LAKESHORE ROAD
BURLINGTON, ONTARIO
L7R 4A6
416-336-4610
Kent.Novakowski@CCIW.ca

For submission to:
WATER RESOURCES RESEARCH

May, 1996

MANAGEMENT PERSPECTIVE

Title: **MEASUREMENT OF THE HYDRAULIC PROPERTIES OF LOW-PERMEABILITY ROCK.**

Author(s): K. Novakowski and G. Bickerton

NWRI Publ. #:

Citation: Submitted to Water Resources Research

EC Priority/Issue: Selection of possible sites for the location of nuclear waste repositories strongly depends on the reliability of the estimates of the permeability of the host rock. In the case of the Canadian Nuclear Fuel Waste Management Program, a specific target for permeability has been set, above which the site is not acceptable as a repository location. The target permeability is, of course, very small so that the migration of radionuclides to local structural features such as faults will be limited. Unfortunately, measuring the permeability of low-permeability rock is very difficult, both experimentally and by way of interpretation. In this paper, a semi-analytical model is presented which accounts for many of the processes which might influence a hydraulic test conducted in low-permeability rock. Problems related to the non-uniqueness of the test results are investigated. It is concluded that although it may be possible to accurately measure permeability by properly accounting for the appropriate test processes, it is more likely that errors in permeability on the order of one magnitude or greater are more common. Differences in average permeability of one order of magnitude might mean the difference between the acceptance or rejection of a possible repository location.

Environment Canada is responsible for reviewing the concept of deep geological disposal of nuclear waste and this issue may ultimately become very significant in the acceptance of a given repository site.

Current Status: The model developed for this study is relatively unique. Presently, hydrogeologists investigating potential repository sites, worldwide, are using less sophisticated methods without the error estimation.

Next Steps: Study is complete. Model may be marketed. Value estimated at approximately $20K per copy.

ABSTRACT

Hydraulic tests conducted in low-permeability media are subject to numerous influences and processes, many of which manifest in a non-unique fashion. To explore the accuracy and meaning of the interpretation of hydraulic tests conducted under such conditions, a semi-analytical model is developed in which finite skin, double porosity, fractional flow processes, variable wellbore storage, temperature, and test method are considered. Results show that slug test results are normally non-unique when conducted in material of low-permeability. The interpretation can be improved only for the case of finite skin, and only at the cost of significantly increased test duration, by conducting the test using an open-hole period followed by a shut-in period (similar to a drill stem test). In practical terms, using existing testing methods, a degree of uncertainty in transmissivity ranging from a small factor to several orders of magnitude can be anticipated depending on the test method and the interpretive model used. The uncertainty is case specific and must be defined by using the range of possible models.

INTRODUCTION

As part of the process of the siting of hazardous waste facilities such as nuclear waste repositories, investigations are undertaken on the viability of the geological environment to host such wastes. The decision to accept a given geological environment is usually based on the ability of the medium to limit groundwater flow. Thus, measurements of the in-situ permeability of such environments must be carefully conducted so as to provide reliable estimates of groundwater flux and velocity. Errors in these measurements could lead to significant misinterpretation of the viability of a given waste facility.

Measuring the hydraulic properties of media of lower permeability (eg. hydraulic conductivity $< 10^{-10}$ m/s) is usually conducted in-situ under shut-in conditions where a small pulse of water is instantaneously injected or withdrawn from an isolated length of borehole (*Bredehoeft and Papadopolus*, 1980; *Neuzil*, 1982). Under shut-in conditions, there is no free-water surface present in the testing apparatus, thus the transient storage of water in the borehole is very small. This significantly shortens the test duration and diminishes the radius of influence relative to slug tests conducted under open-hole conditions. Slug tests conducted under open-hole conditions in low-permeability material may take many months to complete (*Novakowski*, unpublished data) whereas tests conducted under shut-in conditions may require only hours to complete in rock of similar permeability (eg. *Pickens et al.*, 1987).

During the drilling of boreholes in rocks of low-permeability, drill cuttings or drilling mud may invade the formation resulting in a zone of reduced permeability immediately adjacent to the borehole (*Earlougher*, 1977). This is known as a skin zone and in the case where drilling mud is used to lubricate the drilling process, the skin zone develops as a filter cake (*Abboud and Corapcioglu*, 1993). More commonly, particularly in crystalline rock, drill cuttings invade the

microcracks and open pores, clogging the pathways that form the bulk of the rock permeability. Unlike the filter cake, the outer boundary of the skin zone in this case, is poorly defined. To account for this in the interpretation of hydraulic tests, the skin zone may be represented as a zone of infinitesimal thickness (*Sageev and Ramey*, 1986) or of finite thickness (*Moench and Hsieh*, 1985; *Novakowski*, 1989). For hydraulic tests conducted in low-permeability rock, where the radius of influence is small relative to the scale of the borehole, accounting for a skin zone of finite thickness is most representative.

When conducting hydraulic tests in sparsely-fractured rocks of low-permeability, the exchange of fluid between the fractures and the unfractured rock may influence the results of the test. This is known as double porosity and is accentuated during slug tests conducted under shut-in conditions where a minimal volume of water is injected or withdrawn. There are several analytical models for slug tests which account for dual porosity (*Dougherty and Babu*, 1984; *Sageev and Ramey*, 1986), however, none account for the additional effects of a skin zone of finite thickness.

The traditional assumption that flow to or from a borehole occurs in a uniformly radial pattern during a hydraulic test, has been recently challenged. *Barker* (1988) developed a more generalized model for n-dimensional radial flow. The governing equation for this model is based on the radial flow equation where r is raised to a nonintegral value which may range from 1.0 to 3.0. Both infinitesimal skin and dual porosity were incorporated for constant-rate pumping tests, slug tests, and sinusoidal tests. It was concluded that the interpretation of slug tests is independent of dimension (nonunique results are produced for different dimensions).

Non-uniqueness among slug test models has long been recognized as a limiting factor in the interpretation of field results (*Barker and Black*, 1983; *Dougherty and Babu*, 1984). For

example, each of the processes described above may manifest in the test data in a similar fashion. *Karasaki* (1990) suggested that by prematurely terminating an open-hole slug test and interpreting the following shut-in period, a more reliable and unique estimate of the hydraulic properties of the formation is obtained. This concept was originally developed by *Corea and Ramey* (1986, 1987) for rigorous interpretation of Drill Stem Tests (DSTs), a standard well-testing technique used in the petroleum industry. In the case of low-permeability media, the open-hole period is effectively of constant hydraulic head and simply acts to increase the radius of influence of the hydraulic test to which the following shut-in period will be sensitive.

The objective of this paper is to extend the work of *Barker and Black* (1983) to conditions more typical of those encountered when conducting hydraulic tests in media of low permeability. To achieve this, the use of shut-in slug tests and DSTs in determining unique and accurate estimates of the hydraulic properties of low-permeability media is explored. The models are developed using the Laplace transform technique and additional effects due to changes in temperature and wellbore storage are considered.

MODEL DEVELOPMENT

In the following, the complete boundary value problem for radial flow in the formation is developed and solved using the Laplace transform method. It is assumed that potential effects due to partial penetration are negated by the use of isolated test sections of substantial length relative to the borehole diameter (*Hayashi et al.*, 1987). The formulation for double porosity follows that of *Barker and Black* (1983). An equation of state for the wellbore is developed independently and solved such that the general solution for the formation can be obtained by direct substitution. The solution method for the formation is similar to that used by *Novakowski*

(1989) for a pumping test conducted in the presence of finite skin. Definition of the dimensionless parameters used in the solutions can be found in the notation.

Radial Flow in the Formation

Flow in the formation for the radial dimension of 2 is given by:

$$\frac{\partial^2 p}{\partial r^2}+\frac{1}{r}\frac{\partial p}{\partial r}=\frac{S}{T}\frac{\partial p}{\partial t} \qquad r_w \le r \le \infty \qquad [1]$$

where p is pressure in the formation, t is time, r is radial distance, r_w is the well radius, S is storativity, and T is transmissivity. For a slug test condition, the mass balance equation for the wellbore, modified from *Cooper et al.* (1967), is given as:

$$2\pi r_w T\left.\frac{\partial p}{\partial r}\right|_{r=r_w}=C\frac{dp_w}{dt}-Cp_0\delta(t-t_0) \qquad [2]$$

where C is the wellbore storage factor, and p_w is the pressure in the well. The solution to [1] according to [2], assuming t_0=0, and an initial condition whereby $p_w(0)$=0, is given in the Laplace domain by:

$$\bar{\bar{p}}_{Dw}(s)=\frac{C_D K_0(\sqrt{s})}{[C_D s K_0(\sqrt{s})+\sqrt{s}K_1(\sqrt{s})]} \qquad [3]$$

The dimensionless pressure in the wellbore is given by $\bar{p}_{Dw}$, s is the Laplace variable, C_D is the dimensionless wellbore storage coefficient, and K_0 and K_1 are modified Bessel functions. This solution will be used in the following development for more complex conditions in the wellbore and formation.

For shut-in conditions, the wellbore storage factor is given by:

$$C=V\beta_T\rho g$$

where V is the volume of the isolated section, β_T is the total compressibility of the fluid and the

borehole instrumentation, and ρg is the specific weight of the borehole fluid.

For radial flow, where finite skin and fractures perpendicular to the orientation of the borehole are present, the following governing equations are required:

$$\frac{\partial^2 p_1}{\partial r^2}+\frac{1}{r}\frac{\partial p_1}{\partial r}=\frac{S_1}{T_1}\frac{\partial p_1}{\partial t}-2n_f\frac{K_1'}{T_1}\frac{\partial p_1'}{\partial z}\bigg|_{z=0} \qquad r_w \le r \le r_s \qquad [4]$$

$$\frac{\partial^2 p_2}{\partial r^2}+\frac{1}{r}\frac{\partial p_2}{\partial r}=\frac{S_2}{T_2}\frac{\partial p_2}{\partial t}-2n_f\frac{K_2'}{T_2}\frac{\partial p_2'}{\partial z}\bigg|_{z=0} \qquad r > r_s \qquad [5]$$

where the subscripts 1 and 2 denote the skin zone and formation, respectively, the skin is of thickness r_s, K' is the hydraulic conductivity of the matrix (skin and formation) in the vertical direction z, and n_f is the number of fractures of identical transmissivity intersecting the wellbore, all of which are equally spaced. The transmissivity used in equations [4] and [5] represents the total transmissivity of the isolated section of the wellbore. The remaining equations required for the general solution of equations [4] and [5] are given in the following:

$$\frac{\partial^2 p_1'}{\partial z^2}=\frac{S_{s1}'}{K_1'}\frac{\partial p_1'}{\partial t} \qquad 0 \le z \le L_n \qquad [6]$$

$$\frac{\partial^2 p_2'}{\partial z^2}=\frac{S_{s2}'}{K_2'}\frac{\partial p_2'}{\partial t} \qquad 0 \le z \le L_n \qquad [7]$$

$$p_1(r,0)=p_2(r,0)=0 \qquad [8]$$

$$p_1(r_s,t)=p_2(r_s,t) \qquad [9]$$

$$T_1 \frac{\partial p_1}{\partial r}\bigg|_{r=r_s} = T_2 \frac{\partial p_2}{\partial r}\bigg|_{r=r_s} \qquad [10]$$

$$\frac{\partial p_1'}{\partial z}\bigg|_{z=L_n} = \frac{\partial p_2'}{\partial z}\bigg|_{z=L_n} = 0 \qquad [11]$$

$$\begin{aligned} p_1(r,t) &= p_1'(0,r,t) \\ p_2(r,t) &= p_2'(0,r,t) \end{aligned} \qquad [12]$$

$$p_1'(z,r,0) = p_2'(z,r,0) = 0 \qquad [13]$$

$$p_2(\infty,t) = 0 \qquad [14]$$

$$p_w(t) = p_1(r_w,t) \qquad [15]$$

where L_n is the half-spacing between the fractures. The solutions to [4-15] for pressure in the skin zone and in the formation are found in terms of the pressure in the well, which is as yet undefined. In dimensionless form, the solutions are given for the skin zone and formation, respectively, as:

$$\bar{p}_{D1}(r_D,z_D,s) = \frac{\bar{p}_{Dw}(s)}{\Delta}[I_0(\phi_1^{1/2} r_D)\Delta_1 - K_0(\phi_1^{1/2} r_D)\Delta_2] \qquad [16]$$

$$\bar{p}_{D2}(r_D,z_D,s) = \frac{\bar{p}_{Dw}(s)\gamma}{\Delta r_{Ds}} K_0(\phi_2^{1/2} r_D) \qquad [17]$$

where $\bar{p}_{D1}$, $\bar{p}_{D2}$, and $\bar{p}_{Dw}$ are dimensionless pressures. I_0 is a modified Bessel function of order zero, and all other dimensionless variables are defined in the notation.

Fractional Flow in the Formation

For the case where the flow in the formation is not perfectly radial, a non-integral formulation of equation [1] is required. Because the non-integral formulation leads to non-integral

dimensionality, dimensionless parameters are not developed. The governing equation for flow in the formation is given by (*Barker*, 1988):

$$\frac{K}{r^{n-1}}\frac{\partial}{\partial r}\left(r^{n-1}\frac{\partial p}{\partial r}\right)=S_s\frac{\partial p}{\partial t} \qquad r_w \le r \le \infty \qquad [18]$$

where n is the dimension of the flow system, K is hydraulic conductivity, and S_s is the specific storage. The solution to [18] in terms of the pressure in the well, is obtained using the continuity condition between the well and formation and is given by:

$$\bar{p}(r,s)=\frac{\bar{p}_w(s)\,r^{\nu}K_{\nu}(\lambda r)}{r_w^{\nu}K_{\nu}(\lambda r_w)} \qquad [19]$$

where K_ν is a modified Bessel function of fractional order, ν is equal to $1\text{-}n/2$ and λ^2 is equal to sS_s/K.

Equations of State for the Wellbore

The equation of state for the wellbore which simulates a DST is obtained using superposition:

$$2\pi r_w T\left.\frac{\partial p}{\partial r}\right|_{r=r_w}=C_1[1-\mathrm{H}(t-\tau)]\frac{dp_w}{dt}+C_2[\mathrm{H}(t-\tau)]\frac{dp_w}{dt}-C_1p_0\delta(t) \qquad [20]$$

where C_1 and C_2 are independent wellbore storage factors for the open-hole and shut-in periods, respectively, τ is the duration of the open-hole period, and H is the Heaviside step function. Equation [20] represents the general case where pressure changes are observed during both the open-hole and shut-in period. For the specific case where the open-hole period is of constant pressure, the first term on the right hand side is eliminated.

When a shut-in slug test is conducted after a long open-hole period, the drift in the shut-in

pressure due to the remnant pressure from the open-hole period will influence the result of the slug test (*Pickens et al.*, 1987). To accommodate this, a variation of equation [20] is used:

$$2\pi r_w T \frac{\partial p}{\partial r}\bigg|_{r=r_w} = C_1[1-\mathrm{H}(t-\tau)]\frac{dp_w}{dt} + C_2[\mathrm{H}(t-\tau)]\frac{dp_w}{dt} - C_1 p_0 \delta(t) - C_2 \sum_{i=1}^{m} p_i \delta(t-t_i) \qquad t_i > \tau \qquad [21]$$

where t_i is the time at which the slug of magnitude p_i is applied. Multiple slug inputs of differing magnitude, can be simulated using equation [21]. The Laplace transform of equation [21], expressed in terms of the dimensionless pressures in the wellbore and formation, is given by:

$$\begin{aligned}\bar{p}_{Dw}(s) = {} & \frac{1}{C_{D2}s}\frac{dp_D}{dr_D}\bigg|_{r_D=1} + \frac{1}{C_{D2}s}(C_{D2}-C_{D1})p_{Dw}(\tau_D)\exp\{-s\tau_D\} \\ & + \frac{1}{C_{D2}}(C_{D2}-C_{D1})\int_0^{\tau_D}\exp\{-st_D\}p_{Dw}(t_D)\,dt_D \\ & + \frac{C_{D1}}{C_{D2}s} + \frac{1}{s}\sum_{i=1}^{n} p_{Di}\exp\{-st_{Di}\}\end{aligned} \qquad [22]$$

Note that equation [22] requires knowledge of p_{Dw} in real space. Since this is unknown, the inversion of equation [3] is used as an approximation, for the uniform flow case. For the case where other solutions (i.e. finite skin) are used with [22], the appropriate solution should also be substituted for p_{Dw}.

Under testing conditions where a gas phase is present in the isolated test interval, the wellbore storage coefficient may become a function of pressure. This is often encountered in petroleum wells where natural gas may form a highly-compressible free phase. Closed-chamber theory has been used to formulate a conceptual model for this problem, and numerical methods are required for simulation due to the non-linear nature of the equation of state (*Mfonfu and Grader*, 1992). When testing in low-permeability rock, the free-phase may arise due to the

entrapment of air during the packer inflation process. Down-hole equipment may also deform in a non-linear fashion, resulting in a variable wellbore storage coefficient.

An alternative to closed-chamber theory is the approach used by *Fair* (1979) and *Hegeman et al.*, (1993), where it is assumed that the variability in the wellbore storage coefficient can be developed as an additional term in the equation of state. In the following example, the pressure term p_c represents the change in pressure due to the change in wellbore storage:

$$2\pi r_w T \left.\frac{\partial p}{\partial r}\right|_{r=r_w} = C\left\{\frac{dp_w}{dt} - \frac{dp_c}{dt}\right\} - Cp_0\delta(t) \qquad [23]$$

where C is the wellbore storage coefficient as before. The expression for p_c can be given a functional form of any type provided that the function can be Laplace transformed. In the example provided by Fair (1979), an exponential function was used:

$$p_c(t) = C_w(1 - \exp\{-t/\alpha_c\}) \qquad [24]$$

where C_w is a constant which determines the magnitude of the change in wellbore storage and the constant α_c determines the rate at which the pressure changes due to changes in the wellbore storage. The forward Laplace transform of [23] and [24] results in (in dimensionless form):

$$\bar{p}_{Dw}(s) = \frac{1}{C_D s}\left.\frac{d\bar{p}_D}{dr_D}\right|_{r_D=1} + \frac{C_{Dw}}{s}\left[1 - \frac{s}{s + 1/\alpha_{Dc}}\right] + \frac{1}{s} \qquad [25]$$

where C_{Dw} and α_{Dc} are defined in the nomenclature.

A similar approach can be used to account for changes in the wellbore pressure due to changes in down-hole temperature. Changes in borehole temperature can result in significant departures from the ideal response to a hydraulic test conducted in very-low-permeability material (*Pickens et al.*, 1987). Such changes can arise due to differences between the drilling fluid

temperature and formation temperature (*Pickens et al.*, 1987) or through heat conduction and/or heat development in the borehole instrumentation (*Beauheim*, 1994). To account for this, the equation of state for the wellbore is formulated to include the change in volume due to change in pressure (i.e. slug input) and the change in volume due to change in temperature. The change in volume due to change in temperature is developed following the derivation of *Bear and Corapcioglu* (1981) for mass conservation in a heated aquifer. The equation of state is given as:

$$2\pi r_w T \frac{\partial p}{\partial r}\bigg|_{r=r_w} = C\frac{dp_w}{dt} - V\lambda_H \frac{dT_t}{dt} - Cp_0\delta(t) \qquad [26]$$

where T_t is temperature, and λ_H is the thermal expansion coefficient for the borehole fluid. Although virtually any function of temperature can be used in [26] (*C. Neville*, 1990, unpublished notes), an exponential function will be employed for the present study. The function has similar form to equation [24] and is given by:

$$T_t(t) = T_m - (T_m - T_i)\exp\left\{-\frac{t}{\alpha_T}\right\} \qquad [27]$$

where T_i is the initial temperature, T_m is the final temperature, and α_T is the rate of temperature change. The initial temperature can be smaller or larger than the final temperature. Combining [26] and [27], the forward Laplace transform is given by:

$$\bar{p}_{Dw}(s) = \frac{1}{C_D s}\frac{d\bar{p}_D}{dr_D}\bigg|_{r_D=1} + \frac{C_{D\lambda}}{C_D s}(T_{Dm}-1)\left[1 - \frac{s}{s+1/\alpha_{DT}}\right] + \frac{1}{s} \qquad [28]$$

where T_{Dm} is the ratio of T_m over T_i, α_{DT} is the dimensionless rate of temperature change, and $C_{D\lambda}$ is the dimensionless coefficient of thermal storage.

In many practical situations, it may be possible to eliminate the effect of changing

wellbore storage (i.e. equation [23]) but very difficult to isolate the test zone from temperature changes. Thus, a useful equation of state can be constructed by combining [21], and [26]:

$$2\pi r_w T \frac{\partial p}{\partial r}\bigg|_{r=r_w} = C_1[1-\mathrm{H}(t-\tau)]\frac{dp_w}{dt} + C_2[\mathrm{H}(t-\tau)]\frac{dp_w}{dt} - V\lambda_H \rho g \frac{dT}{dt'} - C_1 p_0 \delta(t) - C_2 \sum_{i=1}^{n} p_i \delta(t-t_i) \qquad t_i > \tau \tag{29}$$

and the forward Laplace transform is found using [27] and application of the shift theorem:

$$\begin{aligned}\bar{p}_{Dw}(s) = {} & \frac{1}{C_{D2}s}\frac{d\bar{p}_D}{dr_D}\bigg|_{r_D=1} + \frac{1}{C_{D2}s}(C_{D2}-C_{D1})p_{Dw}(\tau_D)\exp\{-s\tau_D\} \\ & + \frac{1}{C_{D2}}(C_{D2}-C_{D1})\int_0^{\tau_D}\exp\{-st_D\}p_{Dw}(t_D)\,dt_D \\ & + \frac{C_{D\lambda}}{C_{D2}s}(T_{Dm}-1)\exp\{-\tau_D s\}\left[1-\frac{s}{s+1/\alpha_{DT}}\right] \\ & + \frac{C_{D1}}{C_{D2}s} + \frac{1}{s}\sum_{i=1}^{n} p_{Di}\exp\{-st_{Di}\}\end{aligned} \tag{30}$$

Equations [29] and [30] are formulated such that the temperature change only has influence on the pressure during the shut-in period. Normally, C_1 predominates the pressure response during the open-hole period and temperature has negligible effect. A complete derivation of the particular solution using equations [4]-[15] and equation [29] is given in the Appendix.

For conditions of fractional flow, the equation of state is developed using hydraulic conductivity and geometric factors b and ξ_n which relate to the linear thickness and spherical surface of the source, respectively. For standard slug test conditions, the equation of state is given as (*Barker*, 1988):

$$Kb^{3-n}\xi_n r_w^{n-1}\frac{\partial p}{\partial r}\bigg|_{r=r_w} = C\frac{dp_w}{dt} - Cp_0\delta(t) \tag{31}$$

The forward Laplace transform of [31], in dimensioned form, is given by:

$$\bar{p}_w(s) = \frac{Kb^{3-n}\xi_n r_w^{n-1}}{Cs} \left.\frac{d\bar{p}}{dr}\right|_{r=r_w} - \frac{p_0}{s} \qquad [32]$$

To find the equations of state for the fractional flow case equivalent to [20], [21], [23], and [26], substitute $Kb^{3-n}\xi_n r_w^{n-1}$ for $2\pi r_w T$. To find the forward Laplace transforms, substitute for the dimensionless variables in [22], [24], and [27].

To develop particular solutions, the derivative with respect to r of equation [16] or [18] is substituted directly into each equation of state. Determination of the solution in real space is achieved using a numerical inversion scheme based on the *DeHoog et al.* (1982) algorithm. In cases where equation [30] is used in conjunction with [16] or [17], equations [16] and [17] are used both prior to and following the point of shut-in. The particular solutions were verified by using at least two methods to solve each problem and by algebraic reduction to less complicated models.

Implementation of the particular solutions was conducted using a double-precision complex formulation of the necessary Bessel functions (*Amos*, 1986). Gauss quadrature is used for numerical integration. Best results were found with 256 Gauss points and the number of terms in the inversion routine set to 32. Instability in the solutions was observed in some cases at either very early or very late time. This is easily avoided by manipulation of the time range for the simulation.

In the discussion to follow, several example simulations are illustrated in comparison to one another. To facilitate the comparison, a numerical optimization scheme following the method described by *Piggott et al.* (1995), was implemented. In each case, one particular solution was

selected as the baseline and the other particular solutions were forced to fit using the optimization scheme. In most cases, only T and S were varied to achieve the fit, although in some, additional parameters were allowed to vary.

RESULTS AND DISCUSSION

During the drilling of a well in low-permeability rock, it is easy to conceptualize how drill cuttings might invade the surrounding pore space to limit the permeability local to the well. Recognising that shut-in slug tests have a very limited radius of investigation, it can be surmised that DSTs might prove to be more effective in detecting the presence of finite -thickness skin simply because the radius of investigation is increased. To explore this, a comparison was conducted between shut-in slug tests and DSTs having various open-hole periods. Figure 1 illustrates the results of slug tests and DSTs conducted where the uniform value of T is equal to 10^{-12} m^2/s and 10^{-14} m^2/s and for the case where a finite skin of 0.1 m thickness is present. The T_2 for the formation ranges to values as much as four orders of magnitude greater than the skin, where the skin is present. A uniform value of S equal to 5×10^{-6}, a well radius equal to 0.0465 m, a casing radius equal to 0.0185 m (riser pipe), and test section length of 10 m was used for all simulations. The radius of the riser pipe and the compressibility of the water were used to calculate C_1 and C_2, respectively. The results are presented in a semi-logarithmic format with dimensionless pressure plotted versus elapsed time in seconds.

Figure 1a illustrates the results of shut-in slug tests conducted under the conditions described above. The effect of the skin of lower permeability is to steepen the dimensionless pressure at late time. The effect is most pronounced where the difference between T_1 and T_2 is only one order of magnitude. Thus, a skin thickness of this magnitude can be detected (provided

this response is unique) using the shut-in slug test method. Unfortunately, for lower values of T, such as the case for $T=10^{-14}$ m^2/s, greater than 10 days test duration are required to collect enough data such that the departure from the uniform medium curve would be observed. In many cases, this test duration would be impractical.

Figure 1b illustrates the results of simulations conducted under conditions identical to Figure 1a, except that the borehole was exposed to an open-hole pressure for a period of 10 days and then shut-in. The effect of the open hole period, is to move forward, in time, the point at which the pressure for a finite skin departs from the curve for a uniform medium. In addition, the early-time portion of the curves for the case where a finite skin of $T=10^{-12}$ m^2/s is present, are distinctively steep and decline over a similar time period to the case for the shut-in slug test. Thus, at this transmissivity there is no real advantage to conducting a DST in favour of a shut-in slug test. At lower transmissivity, conducting the DST is a disadvantage because the effect of the open-hole period extends the duration at which the p_{Dw} remains near unity, rendering the test impractical using standard testing methodologies.

Figure 1c illustrates the extreme case where the open-hole period is extended to 100 days. At higher T, the shape of the curves for finite skin are even more distinctive with a significant break in slope at late time. The shape of the curves in the case of lower T is similar to that for open-hole periods of lesser duration, although the departure from uniform flow occurs at an even earlier point in time. Note that greater than 100 days are required to return to near-equilibrium conditions at a T of 10^{-14}. For standard testing equipment such as described by *Pickens et al.* (1987) which is used only temporarily in a testing borehole, test durations such as this are completely impractical. However, tests of this duration are easily conducted using permanent

casing completions such as that described by *Black et al.*(1987). In this case, the test is conducted by opening access ports to one or more intervals and exposing these to the casing water level for the desired period of time. After closure of the access port, pressure in the isolated interval can be measured continuously or periodically depending on the transmissivity of the formation. Where the T of the interval is low, periodic measurements of interval pressure over extended periods of time will provide enough data to interpret the results for the presence of a finite skin of lower T.

To explore the issue of uniqueness raised above with respect to slug test results, Figure 2a shows the results of a comparison conducted between the particular solutions for finite skin, fractional flow, and a uniform medium. The particular solution for finite skin was used as the baseline case. The values of T_1 and T_2 for the baseline case are 10^{-12} m^2/s and 10^{-11} m^2/s, respectively. Other parameters are identical to that used for Figure 1. The agreement between the solutions is quite good for this combination of parameters, although the errors incurred by using an inappropriate particular solution are not large. For example, the T obtained using the particular solution for uniform flow reflects more closely the value for T_1 than T_2. This is similar to what was observed by *Barker and Black* (1984) for the double porosity case.

Figure 2b illustrates the fit achieved with the solution for uniform flow for the case of a DST where the open-hole period is 10 days. In this case, the agreement between the solutions is poor, although the interpreted value of T more closely reflects the transmissivity of the formation than for the shut-in slug test case. As illustrated in Figure 1b, this is a function of the increased break-in-slope imparted by the presence of the skin. Thus, as observed by *Karasaki* (1990) for open-hole slug tests, the use of a modified DST will also improve on the uniqueness

of the interpretation for finite skin in the shut-in case.

The effect of double porosity is similar to that for finite-thickness skin, i.e. the slope of the recovery curve is steepened. For example, Figure 3a illustrates the case where slug tests are conducted using an isolated test section of 10 m length. The baseline condition is established using the solution for double porosity where the test section is intersected by 20 fractures. The cumulative T and S are as for the previous Figures. The K and S_s for the matrix are 1×10^{-14} m/s and 5×10^{-7} 1/m, respectively. A fit using the solutions for a uniform medium and fractional flow was obtained using only slightly different values than that for the baseline case. Thus, the effect of double porosity is of marginal importance under conditions of low permeability.

It is interesting to note that the non-uniqueness between the solutions for a uniform medium and double porosity is not diminished by conducting a DST (Figure 3b). This is likely because the effect of double porosity on the shape of the recovery curve is so minimal.

Hydraulic tests conducted in low-permeability material are commonly plagued by the effects of changing temperature. Figures 4a and 4b illustrate the effect of a rise in temperature of 0.1° C during a slug test and DST, respectively. In both cases, the effect of temperature manifests in a similar fashion, creating a significant hump in pressure at early time. The case for a finite skin of lower T is also shown. It is interesting to note, however, that in comparison with the similar curves shown in Figures 1a and 1b, the time at which the solution for finite skin diverges from that for a uniform medium is approximately the same. Thus, it is not necessary to eliminate temperature effects from test design when conducting tests in the presence of a finite skin of lower permeability.

Figures 4a and 4b also show the effects of a finite skin of larger permeability than the

formation for the slug and DST case. The inflection point on the curve shown in Figure 4a occurs at the point where the advancing pressure front encounters the lower permeability of the formation. This inflection point does not appear in Figure 4b, which illustrates that the radius of influence is significantly larger for this test relative to the slug test case.

The solution for fractional flow was found to fit well to the slug test solutions for both finite skin and double porosity (Figures 2a and 3a). Although the equivalent solution for a DST was not coded, it can be surmised that the solution will behave in the same fashion (i.e. fit well to the other solutions). This is because virtually any slope of the recovery curve can be obtained depending on the combination of K, S_s, and n. Data that exhibit strong inflection points at mid-time can not be interpreted using this solution and thus should possess some uniqueness.

Figure 5 illustrates the comparison between the slug test solutions for finite skin and variable wellbore storage. The solution for finite skin was used as the base case and two examples are given, one with a wellbore storage factor, C, slightly greater than water, and the other with C two orders of magnitude greater than water. In both cases, the solution for variable wellbore storage is observed to fit well to the solution for finite skin. Where the skin permeability is greater, the fitted value of T underestimates the true T by one order of magnitude. Conversely, where the skin permeability is smaller, the estimated T is greater by more than ½ an order of magnitude. In both cases S is underestimated. Note that the increased wellbore storage factor results in a significant delay in the initial decline in pressure (compare to Figure 1a). Thus, the discussion above regarding test duration must be tempered considering that it is unlikely to find a testing apparatus that is entirely incompressible. It should also be noted, that because the form of the solutions for variable wellbore storage and temperature effects are so

similar, the manifestation of the solutions will also be similar. In this case, however, it is relatively easy to determine the need for the temperature model, provided temperature measurements from the test section are available.

CONCLUSIONS

A semi-analytical model was developed for hydraulic tests conducted in low-permeability media, in which processes such as finite-thickness skin, double porosity, temperature effects, and variable wellbore storage are considered. The model was formulated to account for hydraulic tests conducted in the traditional slug or pulse test configuration, and where an open-hole period is followed by a shut-in period (similar to a drill stem test). The model was developed using a forward Laplace transform and a numerical scheme for the inversion of the transform. Verification was conducted by finding the solutions through at least two different solution methods.

To investigate the uniqueness of each solution, a comparison was conducted using an inverse formulation of the model. It was shown that the effect of finite-thickness skin, double porosity, fractional flow, variable wellbore storage, and temperature (by analogy), can all manifest in slug test data in a virtually identical fashion. In some cases, it may be possible to determine the appropriate model by using geological data (i.e. known presence of fractures), or measurements of the testing apparatus (i.e. equipment compliance). More commonly, however, uncertainty of some magnitude must expected in any interpretation of this type of test when conducted in a low-permeability environment. Definition of the degree of uncertainty could be informally undertaken by inverting all possible models to the data set. More rigorous definition could be undertaken using stochastically defined parameter sets with each model.

Where a finite skin is present, it may be possible to improve the detection of the skin and resolve the transmissivities of the skin and formation by conducting the hydraulic test in a DST format. However, this is only practical under conditions where test durations of several months are acceptable. For some testing environments, such as in boreholes completed with permanent multi-packer casing, this is easily conducted. Resolution of other effects such as double porosity are not improved by conducting the test in a DST format.

ACKNOWLEDGEMENTS

The authors are grateful to Chris Neville for providing his notes on the solution of the non-isothermal slug test problem.

NOTATION

b	extent of flow region (refer to *Barker*, 1988)
C	wellbore storage factor, πr_w^2 for open borehole, $V\beta_T \rho g$ for shut-in borehole, L^2.
C_1, C_2	wellbore storage factor [open borehole (πr_w^2), shut-in borehole ($V\beta_T \rho g$)], L^2.
C_D	dimensionless wellbore storage coefficient, $C/2\pi r_w^2 S$.
C_{D1} , C_{D2}	dimensionless wellbore storage coefficient, $C/2\pi r_w^2 S_1$.
C_{Dw}	dimensionless pressure parameter, C_w/p_o.
$C_{D\lambda}$	dimensionless coefficient of thermal storage. $V\lambda_H T_i \rho g/2\pi r_w^2 S\, p_o$.
C_w	variable wellbore storage pressure parameter, M/LT.
g	gravitational acceleration, L/T^2.
H	Heaviside's unit step function.
I_ν	modified Bessel function of the first kind and order ν.
K	hydraulic conductivity of the formation, L/T.
K'_1 , K'_2	hydraulic conductivity of the matrix (skin, formation), L/T.
K_ν	modified Bessel function of the second kind and order ν.
L	dimensionless half spacing between fractures, L_n/r_w.
L_n	half spacing between fractures, L.
n	dimension of the fracture flow system.
n_f	number of equally spaced fractures of identical transmissivity.
m	number of slugs.
p, p_2	pressure in the formation (skin absent, skin present), M/LT.

p_1	pressure in the skin, *M/LT*.
p'_1, p'_2	pressure in the matrix (skin, formation), *M/LT*.
p_D, p_{D2}	dimensionless pressure in the formation [skin absent (p/p_o), skin present (p_2/p_o)].
p_{D1}	dimensionless pressure in the skin, p_1/p_o.
p'_{D1}, p'_{D2}	dimensionless pressure in the matrix [skin (p_{D1}/p_o), formation (p_{D2}/p_o)].
p_{Di}	dimensionless pressure of slug i, p_i/p_o.
p_{Dw}	dimensionless pressure in the well, p_w/p_o.
$\bar{p}_{Dw}$	dimensionless pressure in the well, Laplace domain.
p_c	change in pressure due to change in wellbore storage, *M/LT*
p_i	pressure of slug i, *M/LT*.
p_o	initial pressure, *M/LT*.
p_w	pressure in the well, *M/LT*.
r	radial distance, *L*.
r_D	dimensionless radial distance, r/r_w.
r_{Ds}	dimensionless skin radius, r_s/r_w.
r_s	skin radius, *L*.
r_w	well radius, *L*.
s	Laplace variable.
S, S_2	storativity of the formation (skin absent, skin present), dimensionless.
S_1	storativity of the skin, dimensionless.
S'_s	specific storage of the formation, L^{-1}.
S'_{s1}, S'_{s2}	specific storage of the matrix (skin, formation), *L/T*.

t	time, T.
t'	$t - \tau$, T.
t_D	dimensionless time, $T_1\ t / S_1 r_w^2$.
t_i	time at which slug i is applied, T.
T, T_2	transmissivity of the formation (skin absent, skin present), L^2/T.
T_1	transmissivity of the skin, L^2/T.
T_{Dm}	ratio of the final temperature over the initial temperature, T_m / T_i.
T_i	initial temperature, °C.
T_m	final temperature, °C.
T_T	temperature, °C.
ν	order of Bessel function.
V	volume of the isolated section, L^3.
z	vertical distance, L.
z_D	dimensionless vertical distance, z/r_w.
α	ratio of the storativity of the formation over the storativity of the skin, S_2/S_1.
α_C	rate at which wellbore storage is modified, T.
α_{DC}	dimensionless rate at which wellbore storage is modified, $T\ \alpha_C\ /\ r_w^2 S$.
α_{DT}	dimensionless rate of temperature change, $T\ \alpha_T\ /\ r_w^2 S$.
α_T	rate of temperature change, T.
β_T	total compressibility of the fluid and borehole instrumentation, LT^2/M.
γ	ratio of the transmissivity of the formation over the transmissivity of the skin, T_1/T_2.

γ_e	$C_D - C_{Di}$.
δ	Dirac function.
Δ	$I_0(\sqrt{\Phi_1})\Delta_1 - K_0(\sqrt{\Phi_1})\Delta_2$.
Δ_1	$\gamma\sqrt{\Phi_1}K_0(\sqrt{\Phi_2}r_{Ds})K_1(\sqrt{\Phi_1}r_{Ds}) - \sqrt{\Phi_2}K_0(\sqrt{\Phi_1}r_{Ds})K_1(\sqrt{\Phi_2}r_{Ds})$.
Δ_2	$\gamma\sqrt{\Phi_1}K_0(\sqrt{\Phi_2}r_{Ds})I_1(\sqrt{\Phi_1}r_{Ds}) - \sqrt{\Phi_2}I_0(\sqrt{\Phi_1}r_{Ds})K_1(\sqrt{\Phi_2}r_{Ds})$.
λ	sS_s/K.
λ_H	thermal expansion coefficient of borehole fluid, $°C^{-1}$.
ξ_n	area of a unit sphere in n dimensions, $2\pi^{n/2}/\Gamma(n/2)$.
ρ	fluid density, M/L^3.
τ	duration of the open-borehole period, T.
τ_D	dimensionless duration of the open-borehole period, $T_1\tau/S_1r_w^2$.
ϕ_1	$s + \omega_1\sqrt{\psi_1 s}\tanh\left(\sqrt{\psi_1 s}L\right)$.
ϕ_2	$\alpha\gamma s + \omega_2\sqrt{\psi_2 s}\tanh\left(\sqrt{\psi_2 s}L\right)$.
ψ_1	$S'_{s1}T_1/S_1K'_1$.
ψ_2	$S'_{s2}T_1/S_1K'_2$.
ω_1	$2n_f K'_1 r_w/T_1$.
ω_2	$2n_f K'_2 r_w/T_2$.

APPENDIX: SOLUTION METHOD

The solution method is illustrated by solving [4]-[15] using [29] as the equation of state for the wellbore. The governing equations and associated boundary and initial conditions are first made dimensionless using the groupings provided in the notation. The dimensionless form of the governing equations [4]-[7] are, respectively

$$\frac{\partial^2 p_{D1}}{\partial r_D^2} + \frac{1}{r_D}\frac{\partial p_{D1}}{\partial r_D} = \frac{\partial p_{D1}}{\partial t_D} - \omega_1 \left.\frac{\partial p'_{D1}}{\partial z_D}\right|_{z_D=0} \qquad 1 \le r_D \le r_{Ds} \qquad \text{[A1]}$$

$$\frac{\partial^2 p_{D2}}{\partial r_D^2} + \frac{1}{r_D}\frac{\partial p_{D2}}{\partial r_D} = \alpha\gamma\frac{\partial p_{D2}}{\partial t_D} - \omega_2 \left.\frac{\partial p'_{D2}}{\partial z_D}\right|_{z_D=0} \qquad r_{Ds} < r_D \qquad \text{[A2]}$$

$$\frac{\partial^2 p'_{D1}}{\partial z_D^2} = \psi_1 \frac{\partial p'_{D1}}{\partial t_D} \qquad 0 \le z_D \le L \qquad \text{[A3]}$$

$$\frac{\partial^2 p'_{D2}}{\partial z_D^2} = \psi_2 \frac{\partial p'_{D2}}{\partial t_D} \qquad 0 \le z_D \le L \qquad \text{[A4]}$$

The dimensionless form of the remaining boundary and initial conditions, [8]-[15], are given respectively by

$$p_{D1}(r_D,0) = p_{D2}(r_D,0) = 0 \qquad \text{[A5]}$$

$$p_{D1}(r_{Ds},t_D) = p_{D2}(r_{Ds},t_D) \qquad \text{[A6]}$$

$$\gamma \left.\frac{\partial p_{D1}}{\partial r_D}\right|_{r_D=r_{Ds}} = \left.\frac{\partial p_{D2}}{\partial r_D}\right|_{r_D=r_{Ds}} \qquad [A7]$$

$$\left.\frac{\partial p'_{D1}}{\partial z_D}\right|_{z_D=L} = \left.\frac{\partial p'_{D2}}{\partial z_D}\right|_{z_D=L} = 0 \qquad [A8]$$

$$p_{D1}(r_D,t_D) = p'_{D1}(0,r_D,t_D) \qquad [A9]$$

$$p_{D2}(r_D,t_D) = p'_{D2}(0,r_D,t_D) \qquad [A10]$$

$$p'_{D1}(z_D,r_D,0) = p'_{D2}(z_D,r_D,0) = 0 \qquad [A11]$$

$$p_{D2}(\infty,t_D) = 0 \qquad [A12]$$

$$p_{Dw}(t_D) = p_{D1}(1,t_D) \qquad [A13]$$

Application of the Laplace transform to [A1]-[A4], and the subsequent substitution of the initial conditions [A5] and [A11], leads to the following equations

$$\frac{\partial^2 \bar{p}_{D1}}{\partial r_D^2} + \frac{1}{r_D}\frac{\partial \bar{p}_{D1}}{\partial r_D} - s\bar{p}_{D1} + \omega_1 \left.\frac{\partial \bar{p}'_{D1}}{\partial z_D}\right|_{z_D=0} = 0 \qquad 1 \le r_D \le r_{Ds} \qquad [A14]$$

$$\frac{\partial^2 \bar{p}_{D2}}{\partial r_D^2} + \frac{1}{r_D}\frac{\partial \bar{p}_{D2}}{\partial r_D} - \alpha\gamma s\bar{p}_{D2} + \omega_2 \left.\frac{\partial \bar{p}'_{D2}}{\partial z_D}\right|_{z_D=0} = 0 \qquad r_{Ds} < r_D \qquad [A15]$$

$$\frac{\partial^2 \bar{p}'_{D1}}{\partial z_D^2} - \psi_1 s \bar{p}'_{D1} = 0 \qquad 0 \le z_D \le L \qquad \text{[A16]}$$

$$\frac{\partial^2 \bar{p}'_{D2}}{\partial z_D^2} - \psi_2 s \bar{p}'_{D2} = 0 \qquad 0 \le z_D \le L \qquad \text{[A17]}$$

where the overbar denotes the Laplace transformed parameter and s is the Laplace transform variable. Application of the Laplace transform to the remaining boundary conditions [A6]-[A10] and [A12]-[A13] gives, respectively

$$\bar{p}_{D1}(r_{Ds},s) = \bar{p}_{D2}(r_{Ds},s) \qquad \text{[A18]}$$

$$\gamma \left.\frac{\partial \bar{p}_{D1}}{\partial r_D}\right|_{r_D = r_{Ds}} = \left.\frac{\partial \bar{p}_{D2}}{\partial r_D}\right|_{r_D = r_{Ds}} \qquad \text{[A19]}$$

$$\left.\frac{\partial \bar{p}'_{D1}}{\partial z_D}\right|_{z_D = L} = \left.\frac{\partial \bar{p}'_{D2}}{\partial z_D}\right|_{z_D = L} = 0 \qquad \text{[A20]}$$

$$\bar{p}_{D1}(r_D,s) = \bar{p}'_{D1}(0,r_D,s) \qquad \text{[A21]}$$

$$\bar{p}_{D2}(r_D,s) = \bar{p}'_{D2}(0,r_D,s) \qquad \text{[A22]}$$

$$\bar{p}_{D2}(\infty,s) = 0 \qquad \text{[A23]}$$

$$p_{Dw}(s) = \bar{p}_{D1}(1,s) \qquad \text{[A24]}$$

The derivatives in [A14] and [A15] are obtained by solving the matrix equations [A16] and [A17]. The general solution to [A16] is given by

$$\bar{p}_{D1}' = a_1 \exp\left(\sqrt{\psi_1 s} z_D\right) + b_1 \exp\left(-\sqrt{\psi_1 s} z_D\right) \qquad 0 \le z_D \le L \qquad \text{[A25]}$$

where a_1 and b_1 are arbitrary constants. The constants a_1 and b_1 are found using [A20], [A21] and [A25] to generate two equations with two unknowns. The resulting equations are then solved using Cramer's rule and a_1 and b_1 are then substituted back into [A25]. The resulting derivative, after simplification, is found to be

$$\left.\frac{\partial \bar{p}_{D1}'}{\partial z_D}\right|_{z_D=0} = -\bar{p}_{D1}(r_D,s)\sqrt{\psi_1 s}\,\tanh\left(\sqrt{\psi_1 s} L\right) \qquad \text{[A26]}$$

Similarly, the derivative in [A15] can be shown to be

$$\left.\frac{\partial \bar{p}_{D2}'}{\partial z_D}\right|_{z_D=0} = -\bar{p}_{D2}(r_D,s)\sqrt{\psi_2 s}\,\tanh\left(\sqrt{\psi_2 s} L\right) \qquad \text{[A27]}$$

Substituting [A26] into [A14] and [A27] into [A15] gives

$$\frac{\partial^2 \bar{p}_{D1}}{\partial r_D^2} + \frac{1}{r_D}\frac{\partial \bar{p}_{D1}}{\partial r_D} - \phi_1 \bar{p}_{D1} = 0 \qquad 1 \le r_D \le r_{Ds} \qquad \text{[A28]}$$

$$\frac{\partial^2 \bar{p}_{D2}}{\partial r_D^2} + \frac{1}{r_D}\frac{\partial \bar{p}_{D2}}{\partial r_D} - \phi_2 \bar{p}_{D2} = 0 \qquad r_{Ds} < r_D \qquad \text{[A29]}$$

where

$$\phi_1 = s + \omega_1\sqrt{\psi_1 s}\,\tanh\left(\sqrt{\psi_1 s}L\right) \qquad [A30]$$

$$\phi_2 = \alpha\gamma s + \omega_2\sqrt{\psi_2 s}\,\tanh\left(\sqrt{\psi_2 s}L\right) \qquad [A31]$$

The general solutions to [A28] and [A29] are given by

$$\bar{p}_{D1}(r_D,s) = a_2 I_0(\sqrt{\phi_1}r_D) + b_2 K_0(\sqrt{\phi_1}r_D) \qquad [A32]$$

$$\bar{p}_{D2}(r_D,s) = a_3 I_0(\sqrt{\phi_2}r_D) + b_3 K_0(\sqrt{\phi_2}r_D) \qquad [A33]$$

where a_2, a_3, b_2 and b_3 are arbitrary constants. Using [A23] to bound the solution, [A33] is reduced to

$$\bar{p}_{D2}(r_D,s) = b_3 K_0(\sqrt{\phi_2}r_D) \qquad [A34]$$

Substituting [A33] and [A34] into [A18], [A19] and [A24] produces three equations with three unknowns

$$a_2 I_0(\sqrt{\phi_1}r_{Ds}) + b_2 K_0(\sqrt{\phi_1}r_{Ds}) = b_3 K_0(\sqrt{\phi_2}r_{Ds}) \qquad [A35]$$

$$\gamma a_2\sqrt{\phi_1}I_1(\sqrt{\phi_1}r_{Ds}) - \gamma b_2\sqrt{\phi_1}K_1(\sqrt{\phi_1}r_{Ds}) = -b_3\sqrt{\phi_2}K_1(\sqrt{\phi_2}r_{Ds}) \qquad [A36]$$

$$a_2 I_0(\sqrt{\phi_1}) + b_2 K_0(\sqrt{\phi_1}) = \bar{p}_{Dw}(s) \qquad [A37]$$

Again the constants a_2, b_2 and b_3 are found by solving [A35]-[A37] using Cramer's rule. The constants are then substituted back into the general solution [A32] and [A34]. The resulting solutions, after simplification, are

$$\bar{p}_{DI}(r_D,s) = \frac{\bar{p}_{Dw}(s)}{\Delta}\left[I_0(\sqrt{\Phi_1}r_D)\Delta_1 - K_0(\sqrt{\Phi_1}r_D)\Delta_2\right] \qquad [A38]$$

$$\bar{p}_{D2}(r_D,s) = \frac{\bar{p}_{Dw}(s)\gamma}{\Delta r_{Ds}} K_0(\sqrt{\Phi_2}r_D) \qquad [A39]$$

where

$$\Delta_1 = \gamma\sqrt{\Phi_1}K_0(\sqrt{\Phi_2}r_{Ds})K_1(\sqrt{\Phi_1}r_{Ds}) - \sqrt{\Phi_2}K_0(\sqrt{\Phi_1}r_{Ds})K_1(\sqrt{\Phi_2}r_{DS}) \qquad [A40]$$

$$\Delta_2 = -\gamma\sqrt{\Phi_1}K_0(\sqrt{\Phi_2}r_{Ds})I_1(\sqrt{\Phi_1}r_{Ds}) - \sqrt{\Phi_2}I_0(\sqrt{\Phi_1}r_{Ds})K_1(\sqrt{\Phi_2}r_{DS}) \qquad [A41]$$

$$\Delta = I_0(\sqrt{\Phi_1})\Delta_1 - K_0(\sqrt{\Phi_1})\Delta_2 \qquad [A42]$$

The solution for dimensionless pressure in the well is obtained by substituting the derivative of [A38] into the equation of state for the wellbore [30] and re-arranging for $\bar{p}_{Dw}(s)$. The required derivative is given by

$$\left.\frac{\partial\bar{p}_{DI}}{\partial r_D}\right|_{r_D=1} = \frac{\bar{p}_{Dw}(s)\sqrt{\Phi_1}}{\Delta}\left[I_1(\sqrt{\Phi_1})\Delta_1 + K_1(\sqrt{\Phi_1})\Delta_2\right] \qquad [A43]$$

Substituting [A43] into [30] gives

$$\bar{p}_{Dw}(s) = \frac{\bar{p}_{Dw}(s)\sqrt{\Phi_1}}{\Delta C_{D2} s}\left[I_1(\sqrt{\Phi_1})\Delta_1 + K_1(\sqrt{\Phi_1})\Delta_2\right]$$

$$+ \frac{(C_{D2} - C_{DI})}{C_{D2} s} \; p_{Dw}(\tau)\exp(-s\tau)$$

$$+ \frac{(C_{D2} - C_{DI})}{C_{D2}} \int_0^{\tau} p_{Dw}(t_D)\exp(-st_D)\,dt_D \qquad \text{[A44]}$$

$$+ \frac{C_{D\lambda}(T_{Dm} - 1)}{C_{D2} s}\left[1 - \frac{s'}{s' + 1/\alpha_{DT}}\right]$$

$$+ \frac{1}{s}\sum_{i=1}^{n} p_{Di}\exp(-st_{Di}) + \frac{C_{DI}}{C_{D2} s}$$

re-arranging for $\bar{p}_{Dw}(s)$ provides the final solution

$$\bar{p}_{Dw}(s) = \frac{(C_{D2} - C_{DI})}{\chi C_{D2} s} \; p_{Dw}(\tau)\exp(-s\tau)$$

$$+ \frac{(C_{D2} - C_{DI})}{\chi C_{D2}} \int_0^{\tau} p_{Dw}(t_D)\exp(-st_D)\,dt_D \qquad \text{[A45]}$$

$$+ \frac{C_{D\lambda}(T_{Dm} - 1)}{\chi C_{D2} s}\exp\{-\tau s\}\left[1 - \frac{s}{s + 1/\alpha_{DT}}\right]$$

$$+ \frac{1}{\chi s}\sum_{i=1}^{n} p_{Di}\exp(-st_{Di}) + \frac{C_{DI}}{\chi C_{D2} s}$$

where

$$\chi = 1 - \frac{\sqrt{\Phi_1}}{\Delta C_{D2} S} \left[I_1(\sqrt{\Phi_1})\Delta_1 + K_1(\sqrt{\Phi_1})\Delta_2 \right] \qquad \text{[A46)}$$

REFERENCES

Abboud, N., and M.Y. Corapcioglu, Effect of mud penetration on borehole skin properties, Water Resour. Res., 29(8), 2941-2950, 1993.

Amos, D.E., Algorithm 644: A portable package for Bessel Functions of complex argument and nonnegative order, ACM Trans. Math. Soft., 12(3), 265-273, 1986.

Barker, J.A., A generalized radial flow model for hydraulic tests in fractured rock, Water Resour. Res., 24(10), 1796-1804, 1988.

Barker, J.A., and J.H. Black, Slug tests in fissured aquifers, Water Resour. Res., 19(6), 1558-1564, 1983.

Black, W.H., H.R. Smith, and F.D. Patton, Multiple-level groundwater monitoring with the MP system, In: Proceedings NWWA-AGU Conf. Surface and Borehole Geophysical Methods and Groundwater Instrumentation, NWWA, Dublin, Ohio, 1987.

Bear, J, and M.Y. Corapcioglu, A mathematical model for consolidation in a thermoelastic aquifer due to hot water injection or pumping, Water Resour. Res., 17(3), 723-736, 1981.

Beauheim, R.L., Practical considerations in well testing of low-permeability media, Eos, 75(16), 151, 1994.

Bredehoeft, J.D., and S.S. Papadopulos, A method for determining the hydraulic properties of tight formations, Water Resour. Res., 16(1), 233-238, 1980.

Cooper, H.H., Jr., J.D. Bredehoeft, and S.S. Papadopulos, Response of a finite-diameter well to an instantaneous charge of water, Water Resour. Res., 3(1), 263-269, 1967.

Correa, A.C., and H.J. Ramey, Jr., Combined effects of shut-in and production: solution with a new inner boundary condition, SPE paper 15579, In: Proc., 61st Annual Technical Conference of the Society of Petroleum Engineers, New Orleans, LA, Oct. 5-8, 1986.

Correa, A.C., and H.J. Ramey, Jr., A method for pressure buildup analysis of drillstem tests, SPE paper 16802, In: Proc., 62nd Annual Technical Conference of the Society of Petroleum Engineers, Dallas, TX, Sept. 27-30, 1987.

De Hoog, F. R., J. H. Knight and A. N. Stokes, An improved method for numerical inversion of Laplace transforms, SIAM. J. Sci.Stat.Comput., 3(3), 357-366, 1982.

Dougherty, D.E., and D.K. Babu, Flow to a partially penetrating well in double-porosity reservoir, Water Resour. Res., 20(8), 1116-1122, 1984.

Earlougher, R.C., Jr., Advances in well test analysis, Society of Petroleum Engineers of AIME Special Monograph, Vol. 5., Society of Petroleum Engineers, Richardson, Tex., 1977.

Fair, W.B., Jr., Pressure buildup analysis with wellbore phase distribution, SPE paper 8206, In: Proc., 54th Annual Fall Technical Conference of the Society of Petroleum Engineers, Las Vegas, NV, Sept. 23-26, 1979.

Hayashi, K., T. Ito, and H. Abé, A new method for the determination of in situ hydraulic properties by pressure pulse tests and application to the Higashi geothermal field, J. Geophys. Res., 92(B9), 9168-9174, 1987.

Hegeman, P.S., D.L. Hallford, and J.A. Joseph, Well-test analysis with changing wellbore storage, SPE Formation Evaluation, 8(3), 201-207, 1993.

Karasaki, K., A systematized drillstem test, Water Resour. Res., 2913-2919, 1990.

Mfonfu, G.B.S., and A.S. Grader, An implicit numerical model for the closed-chamber test, SPE Formation Evaluation, 7(2), 185-192, 1992.

Moench, A.F., and P.A. Hsieh, Analysis of slug test data in a well with finite thickness skin, In: Proc. Seventeenth International Congress, Int. Assoc. Hydrogeol., Tucson, Az., Jan., 1985.

Neuzil, C.E., On conducting the modified 'slug' test in tight formations, Water Resour.Res., 18(2), 439-441, 1982.

Novakowski, K.S., A composite analytical model for analysis of pumping tests affected by well bore storage and finite thickness skin, Water Resour. Res., 25(9), 1937-1946, 1989.

Pickens, J.F., G.E. Grisak, J.D. Avis, D.W. Belanger, and M. Thury, Analysis and interpretation of borehole hydraulic tests in deep boreholes: Principles, model development, and applications, Water Resour. Res., 23(7), 1341-1375, 1987.

Piggott, A., T. Huynh, P. Lapcevic, and K. Novakowski, Automated analysis of hydraulic and tracer tests conducted in fractured rock, Hydrogeol. J., in submittal, 1996.

Sageev, A., and H.J. Ramey Jr., On slug test analysis in double-porosity reservoirs, In: Proceedings 61st Annual Technical Conference, SPE, New Orleans, LA, Oct. 5-8, SPE 15479, 1986.

FIGURE CAPTIONS

Figure 1a Comparison of results for shut-in slug tests using the uniform medium and finite skin models. The comparisons are made for $T=T_1=10^{-12}$ m^2/s and $T=T_1=10^{-14}$ m^2/s.

Figure 1b Comparison of results for DSTs using the uniform medium and finite skin models. The comparisons are made for τ = 10 days, $T=T_1=10^{-12}$ m^2/s and $T=T_1=10^{-14}$ m^2/s.

Figure 1c Comparison of results for DSTs using the uniform medium and finite skin models. The comparisons are made for τ = 100 days. $T=T_1=10^{-12}$ m^2/s and $T=T_1=10^{-14}$ m^2/s.

Figure 2a Optimal fits for the fractional flow and uniform medium models to a finite skin baseline case. The comparisons are for the slug test case.

Figure 2b Optimal fit for the uniform medium model to a finite skin baseline case. The comparisons are for DSTs with τ = 10 days.

Figure 3a Optimal fits for the fractional flow and uniform medium models to a double porosity baseline case. The comparisons are for slug tests with baseline parameters $T=10^{-12}$ m^2/s, $S=5 \times 10^{-6}$, $K=10^{-14}$ m/s, and $S_s=5 \times 10^{-7}$ m^{-1}.

Figure 3b Optimal fit for the uniform medium model to a double porosity baseline case. The comparisons are for DSTs with τ = 10 days and baseline parameters $T=10^{-12}$ m^2/s, $S=5 \times 10^{-6}$, $K=10^{-14}$ m/s, $S_s=5 \times 10^{-7}$ m^{-1}, and $C_1=1.08 \times 10^{-3}$ m^2.

Figure 4a Illustration of the potential impact of a positive skin ($T_1 > T_2$) or temperature rise on shut-in slug tests. The comparisons are made with p_o =98040 Pa, $\lambda_H = 4 \times 10^{-4}\ {}^{o}C^{-1}$, and $\alpha_T = 29000$ sec.

Figure 4b Illustration of the potential impact of a positive skin ($T_1 > T_2$) or temperature rise on DSTs. The comparisons are made for $\tau = 10$ days with p_o =98040 Pa, $\lambda_H = 4 \times 10^{-4}\ {}^{o}C^{-1}$, and $\alpha_T = 29000$ sec.

Figure 5 Comparison of the solutions for finite skin and variable wellbore storage for two different values of the wellbore storage factor, C.

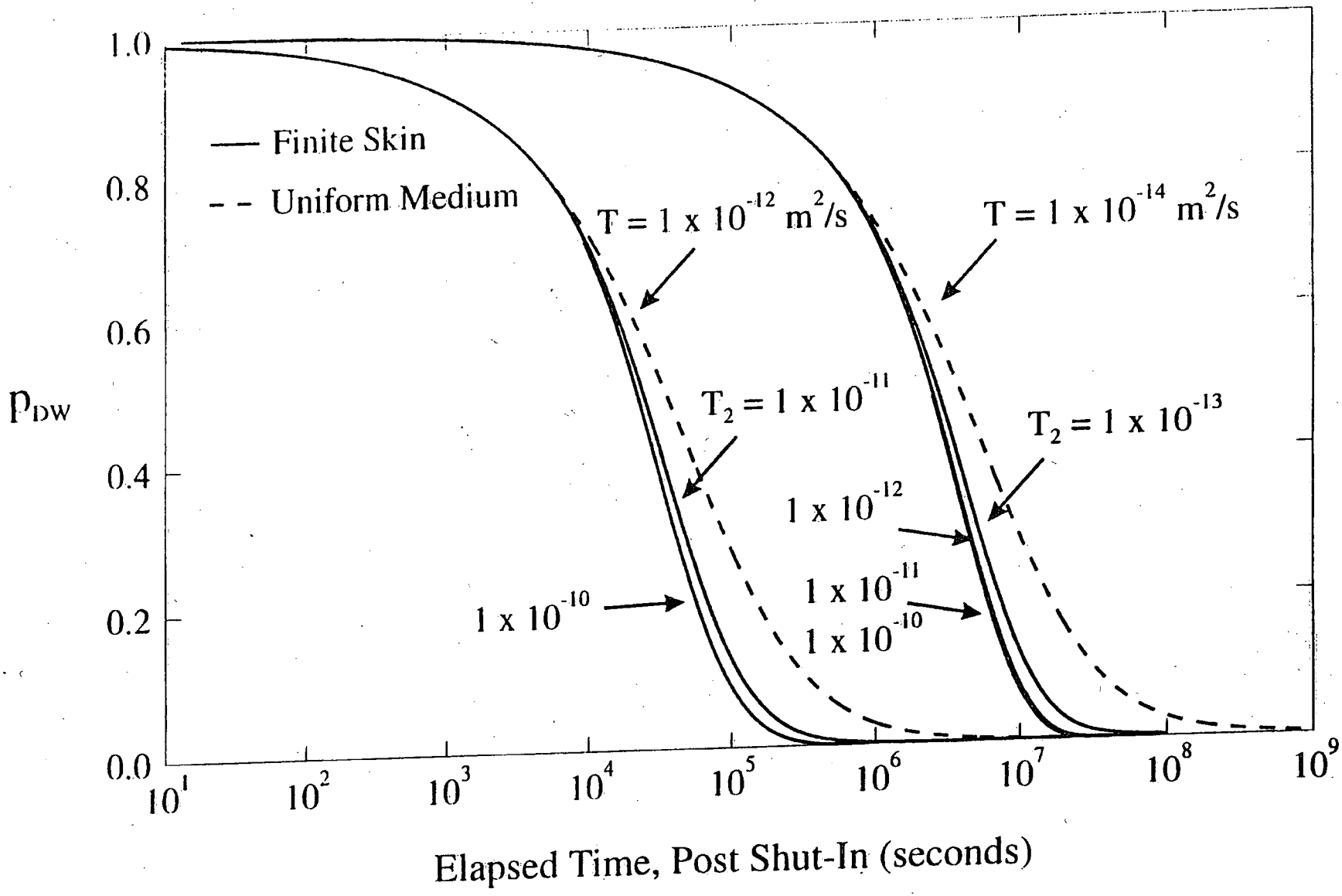

Figure 1a Comparison of results for shut-in slug tests using the uniform medium and finite skin models. The comparisons are made for $T=T_1=10^{-12}$ m²/s and $T=T_1=10^{-14}$ m²/s.

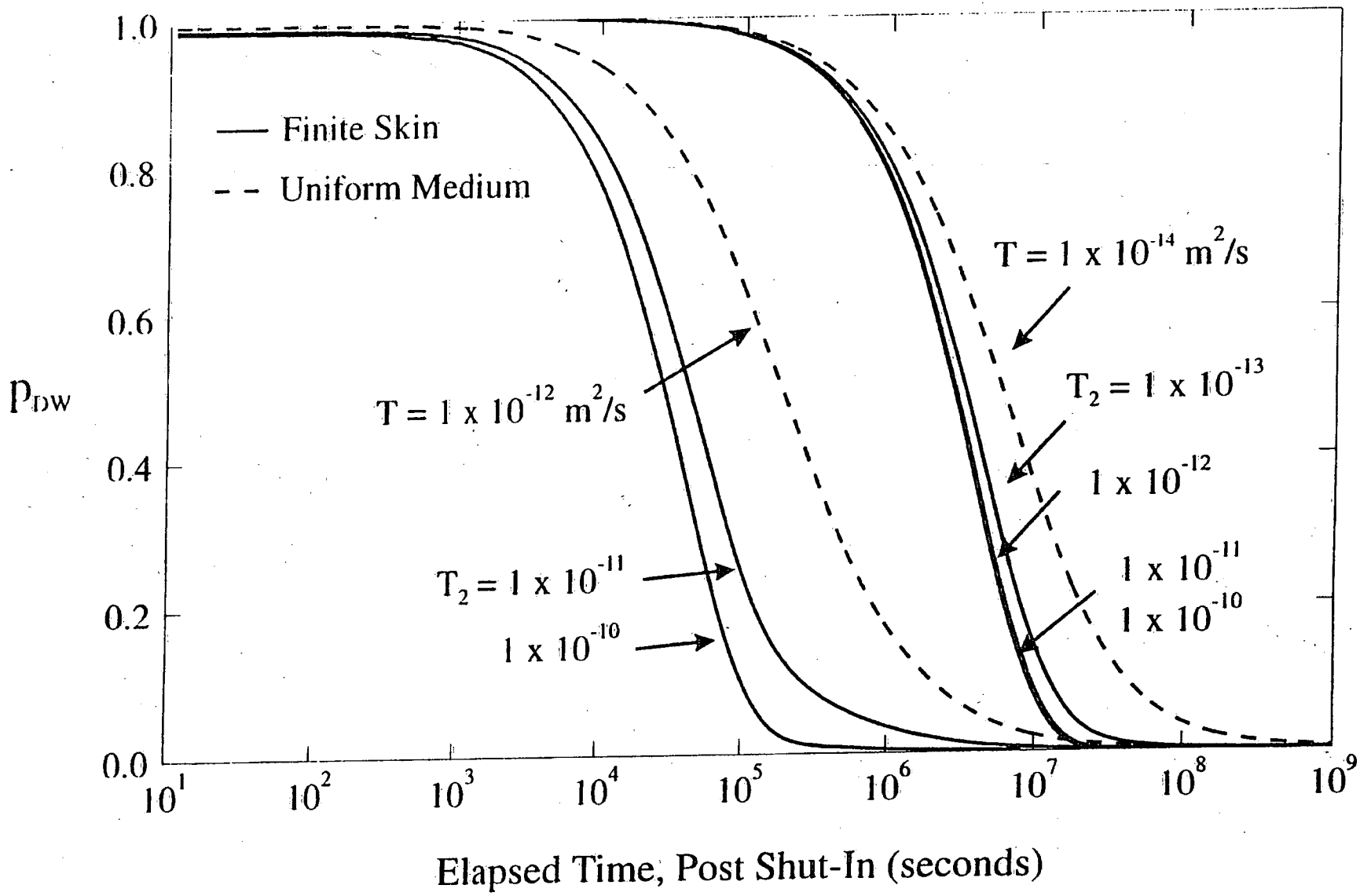

Figure 1b Comparison of results for DSTs using the uniform medium and finite skin models. The comparisons are made for τ = 10 days, $T=T_1=10^{-12}$ m²/s and $T=T_1=10^{-14}$ m²/s.

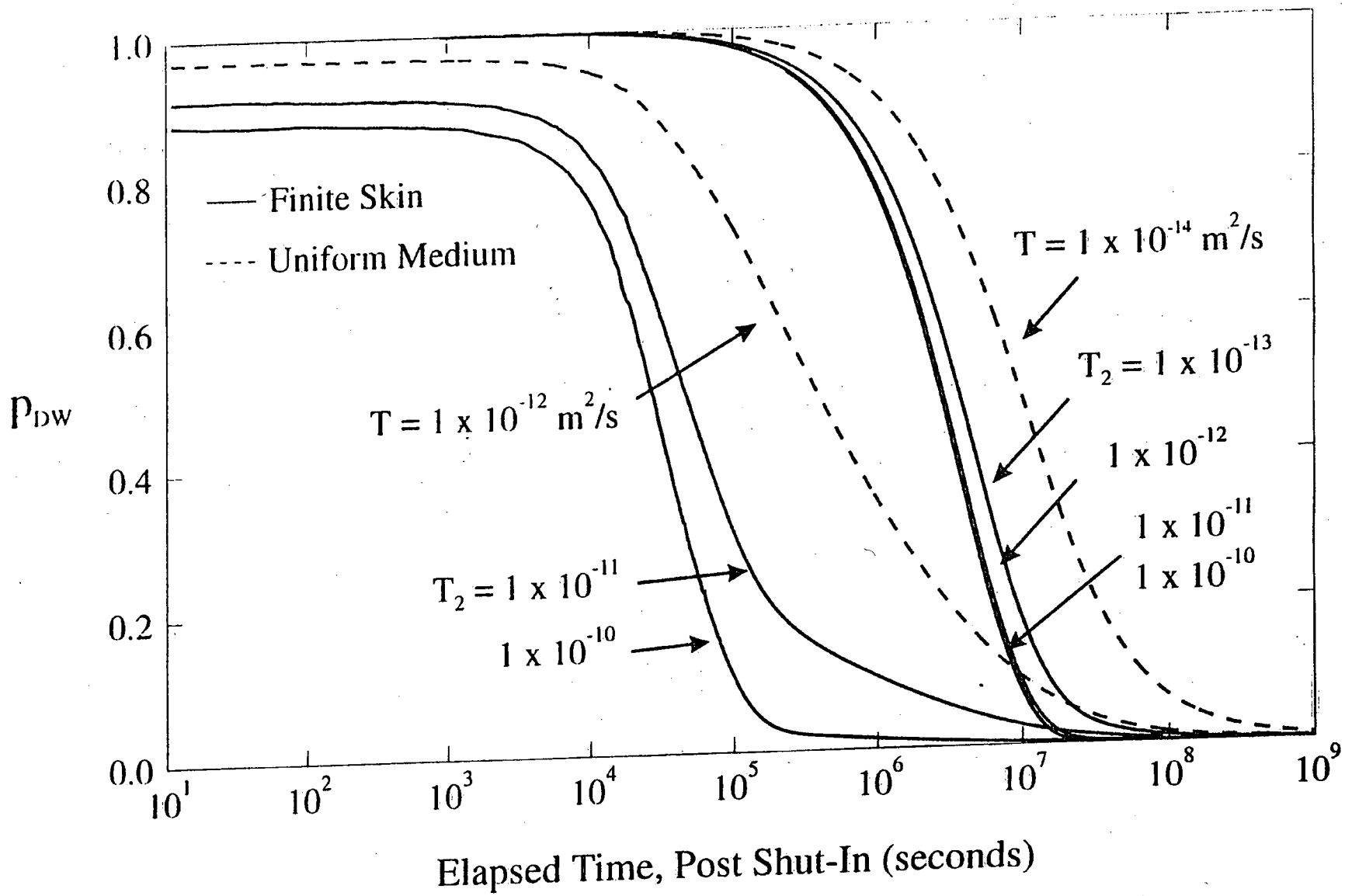

Figure 1c Comparison of results for DSTs using the uniform medium and finite skin models. The comparisons are made for $\tau = 100$ days, $T=T_1=10^{-12}$ m^2/s and $T=T_1=10^{-14}$ m^2/s.

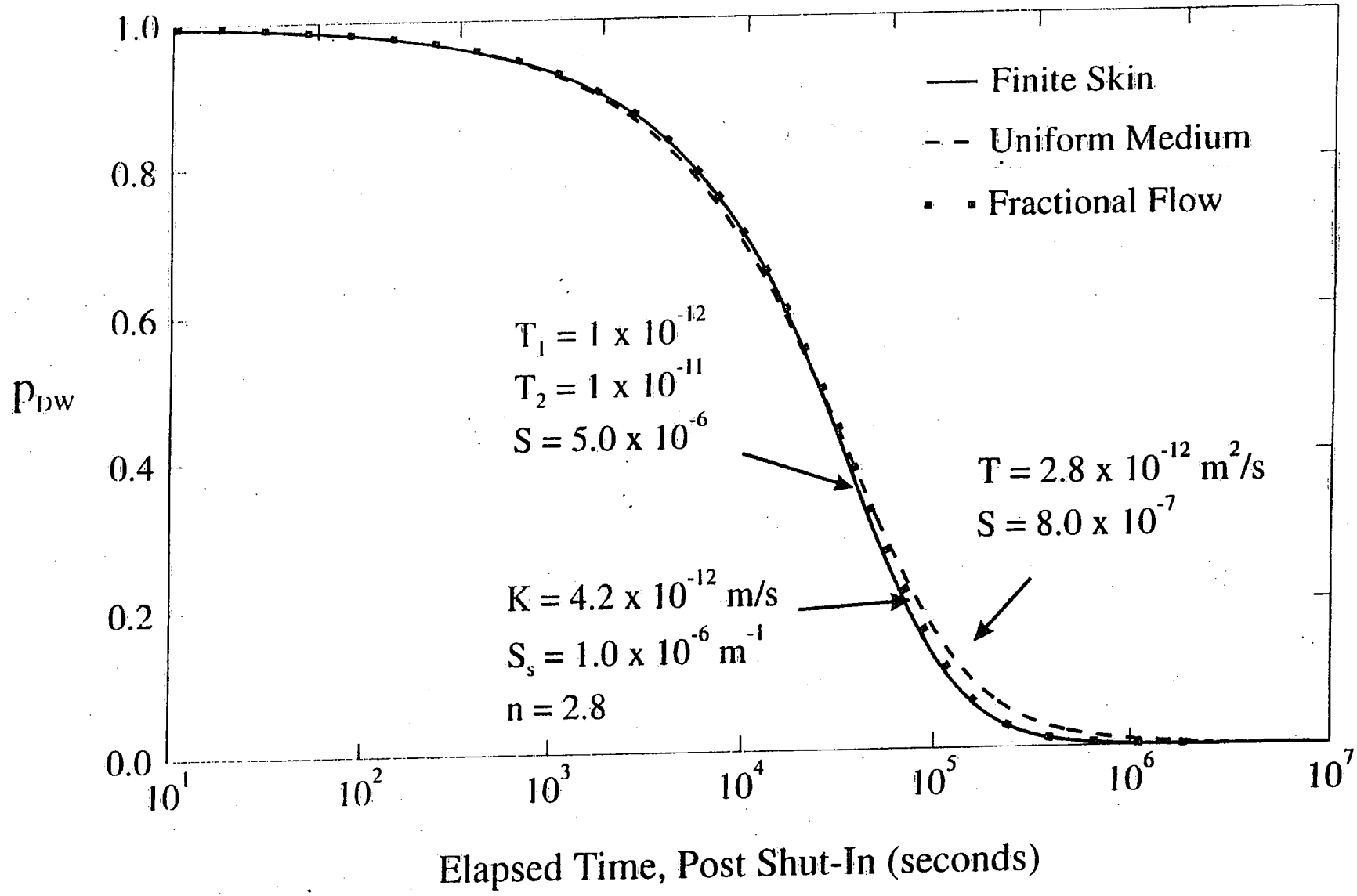

Figure 2a Optimal fits for the fractional flow and uniform medium models to a finite skin baseline case. The comparisons are for the slug test case.

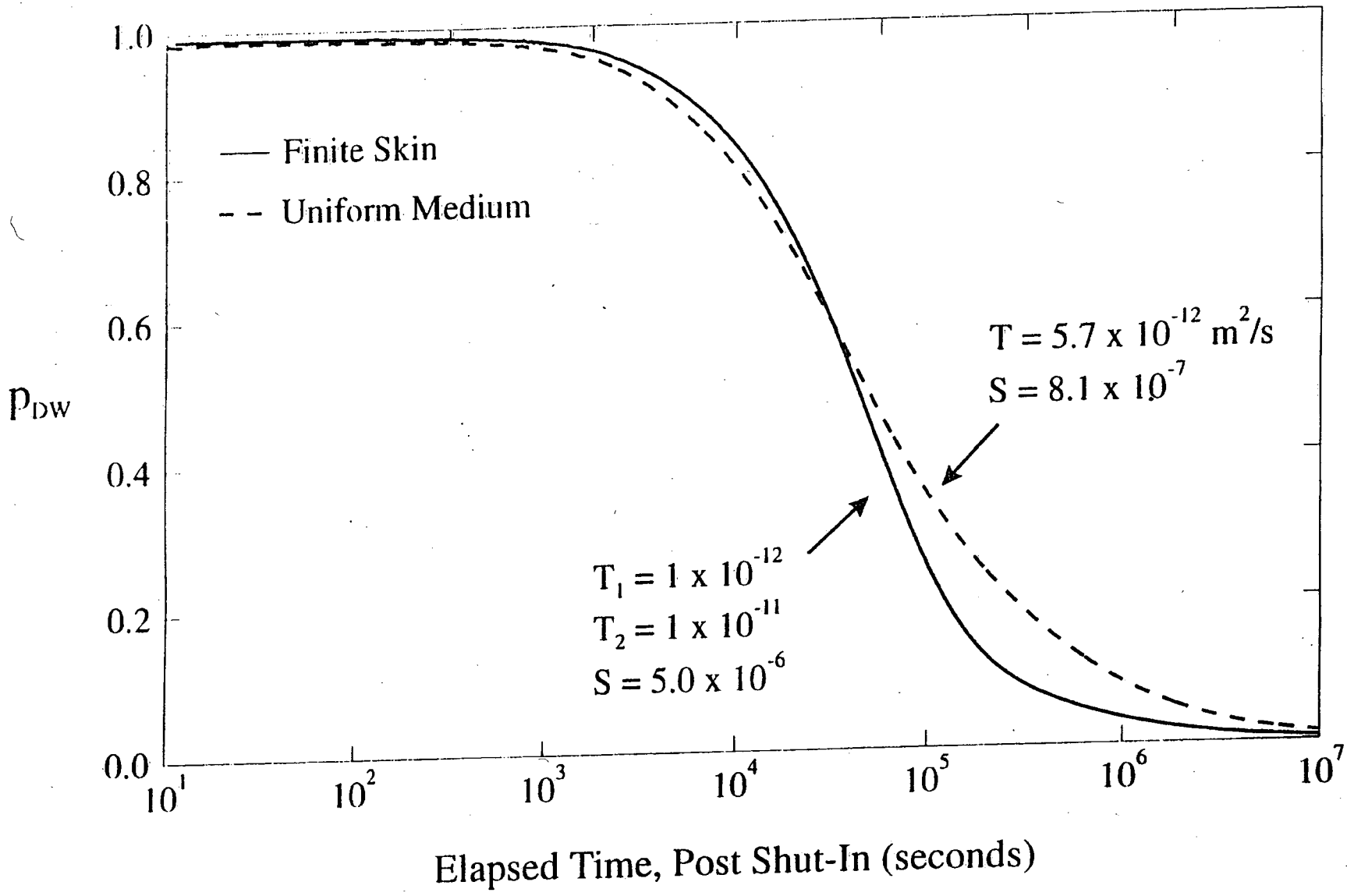

Figure 2b Optimal fit for the uniform medium model to a finite skin baseline case. The comparisons are for DSTs with $\tau = 10$ days.

Novakowski Fig 5a

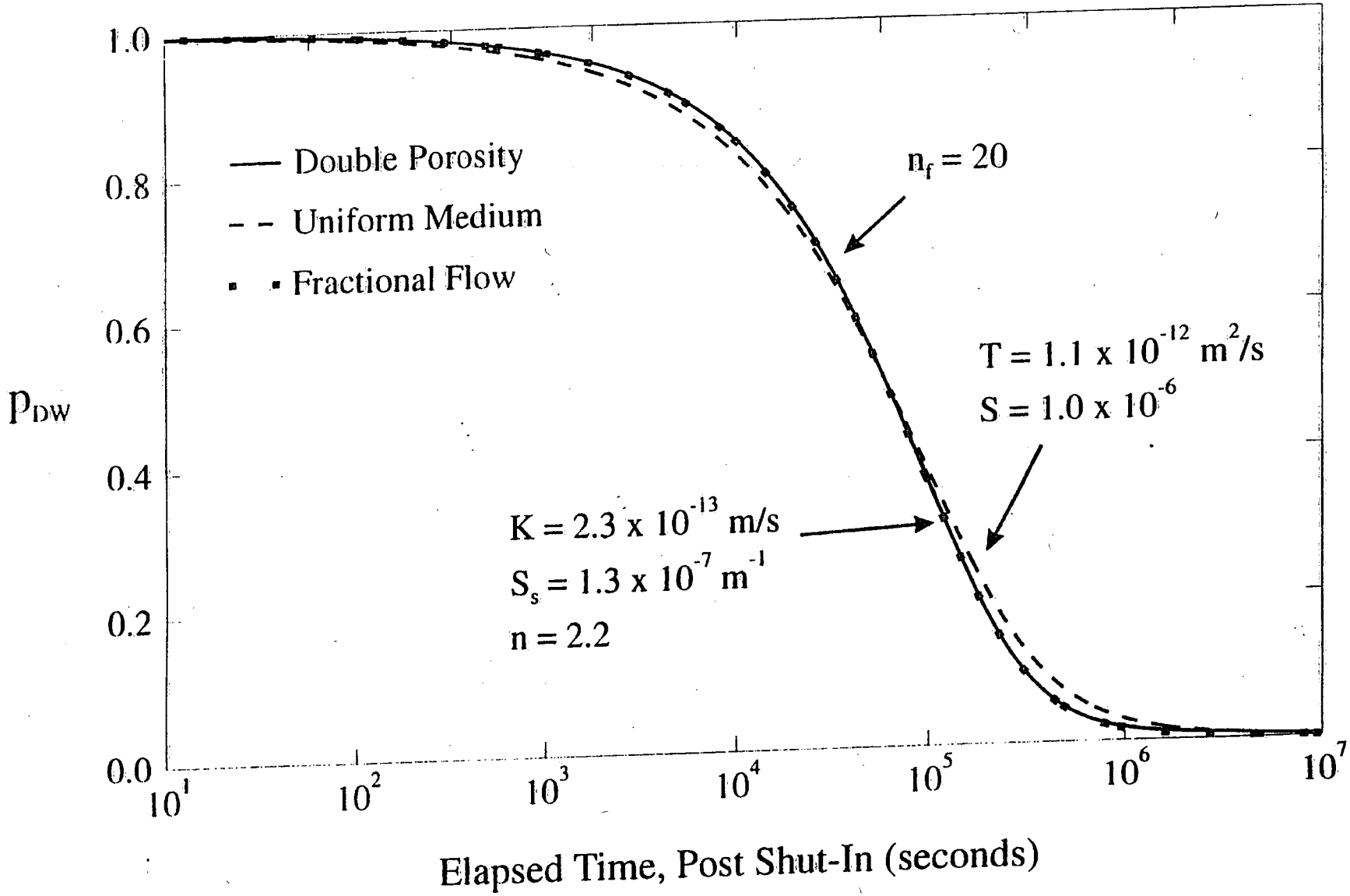

Figure 3a Optimal fits for the fractional flow and uniform medium models to a double porosity baseline case. The comparisons are for slug tests with baseline parameters $T = 10^{-12}$ m^2/s, $S = 5 \times 10^{-6}$, $K = 10^{-14}$ m/s, and $S_s = 5 \times 10^{-7}$ m^{-1}.

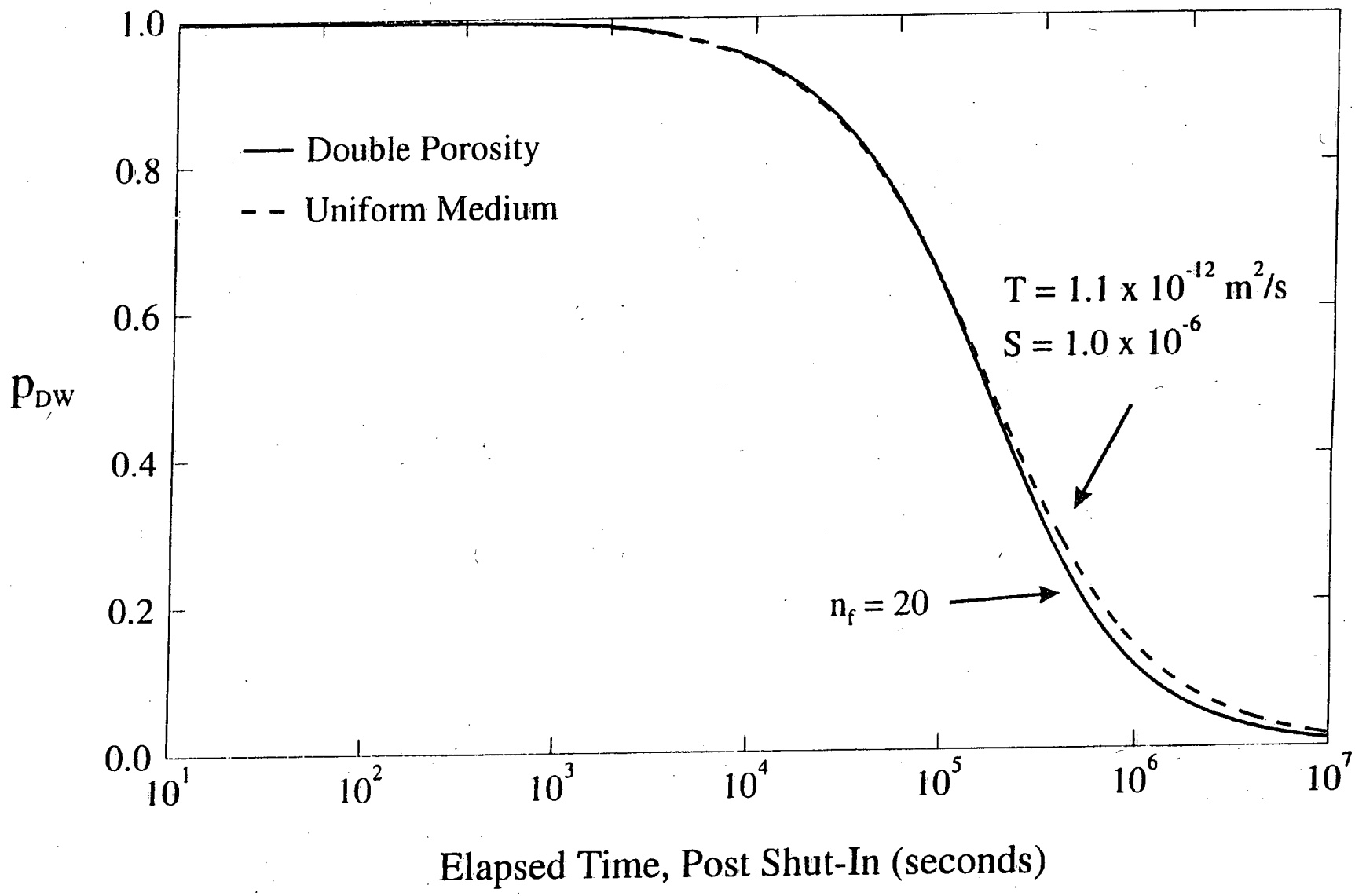

Figure 3b Optimal fit for the uniform medium model to a double porosity baseline case. The comparisons are for DSTs with $\tau = 10$ days and baseline parameters $T = 10^{-12}$ m^2/s, $S = 5 \times 10^{-6}$, $K = 10^{-14}$ m/s, $S_s = 5 \times 10^{-7}$ m^{-1}, and $C_1 = 1.08 \times 10^{-3}$ m^2.

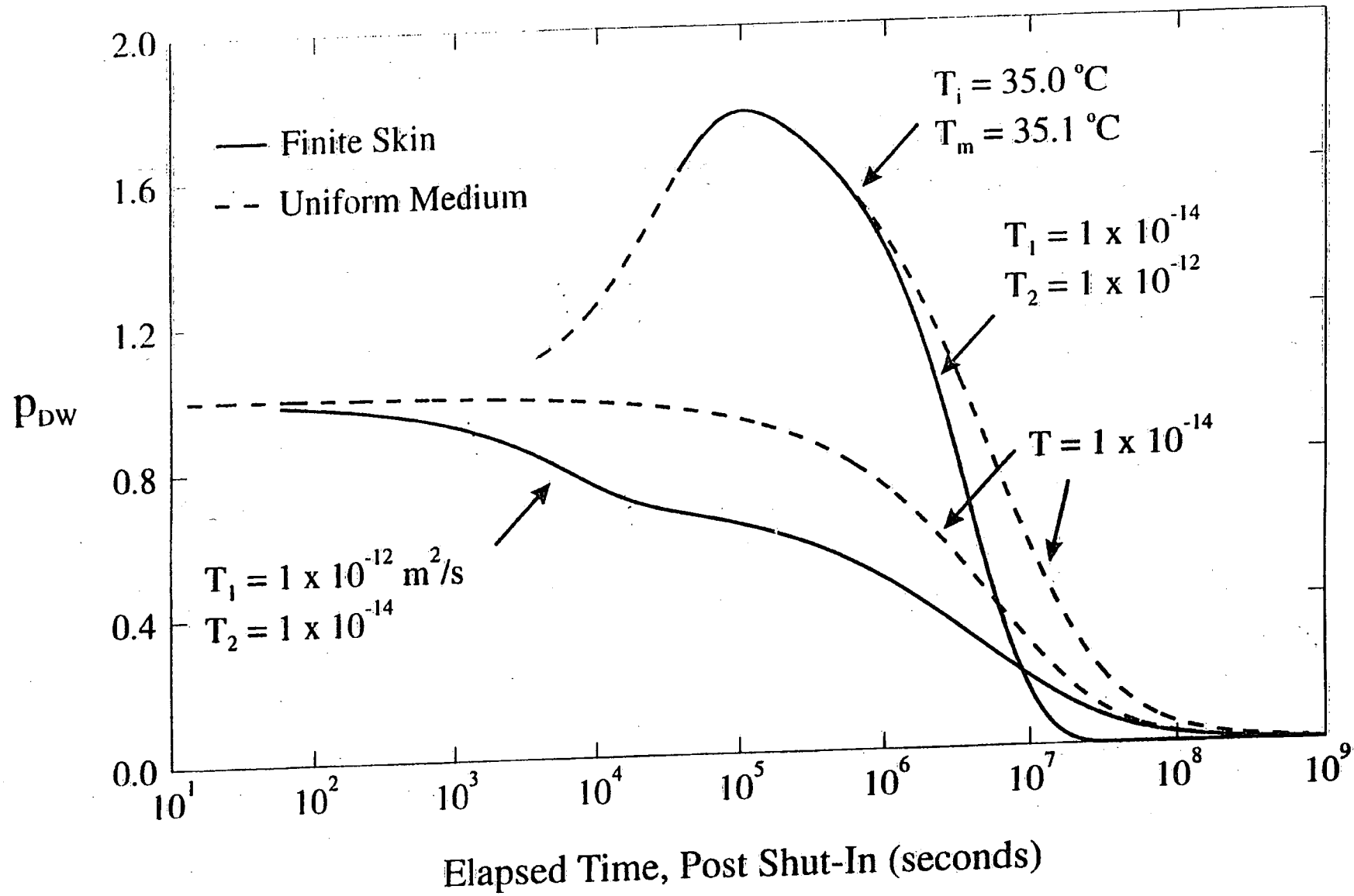

Figure 4a Illustration of the potential impact of a positive skin ($T_1 > T_2$) or temperature rise on shut-in slug tests. The comparisons are made with p_o =98040 Pa, λ_H = 4 x 10^{-4} °C^{-1}, and α_T = 29000 sec.

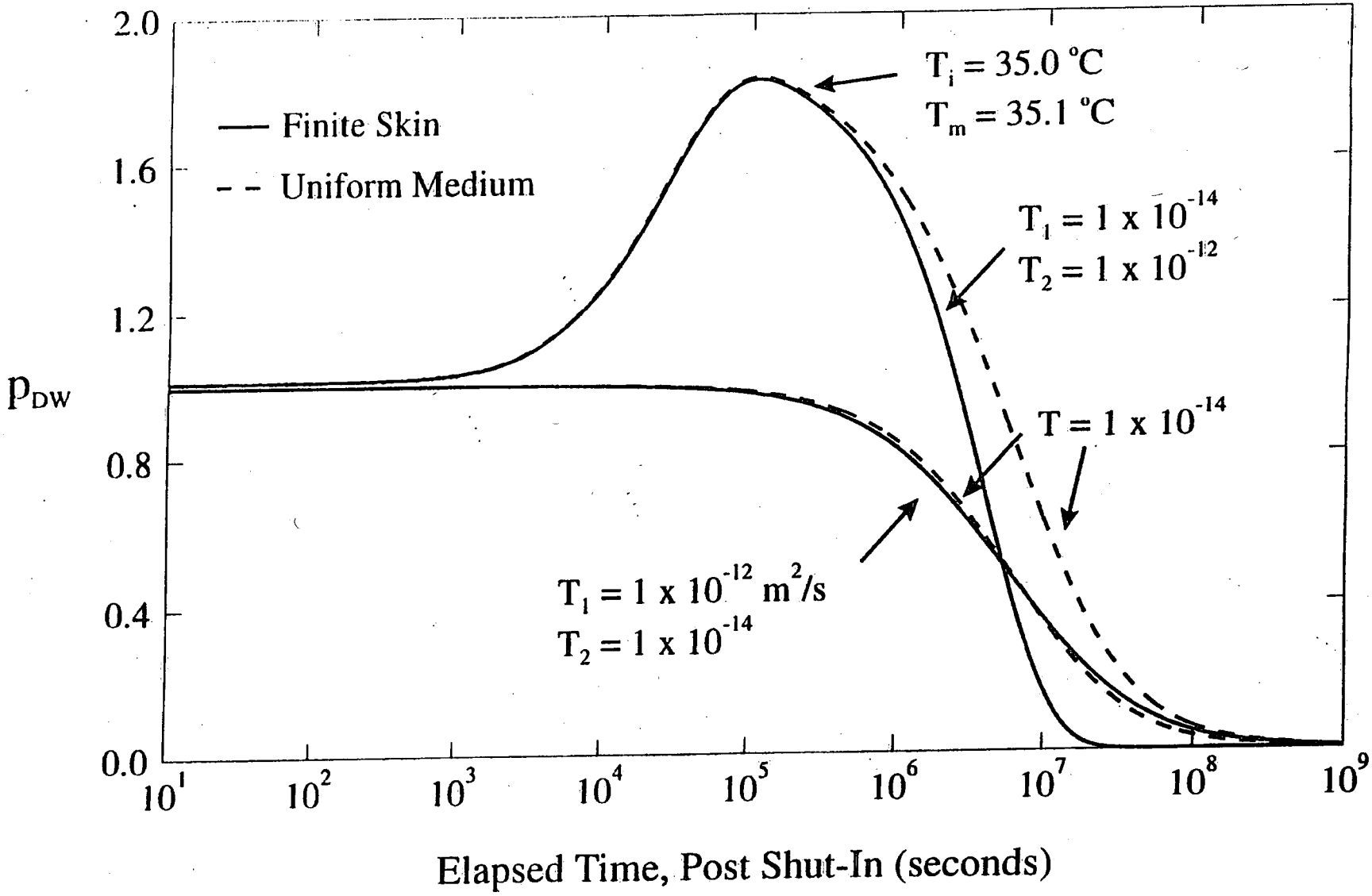

Figure 4b Illustration of the potential impact of a positive skin ($T_1 > T_2$) or temperature rise on DSTs. The comparisons are made for $\tau = 10$ days with $p_o = 98040$ Pa, $\lambda_H = 4 \times 10^{-4}$ °C^{-1}, and $\alpha_T = 29000$ sec.

Novakowski Fig. 5

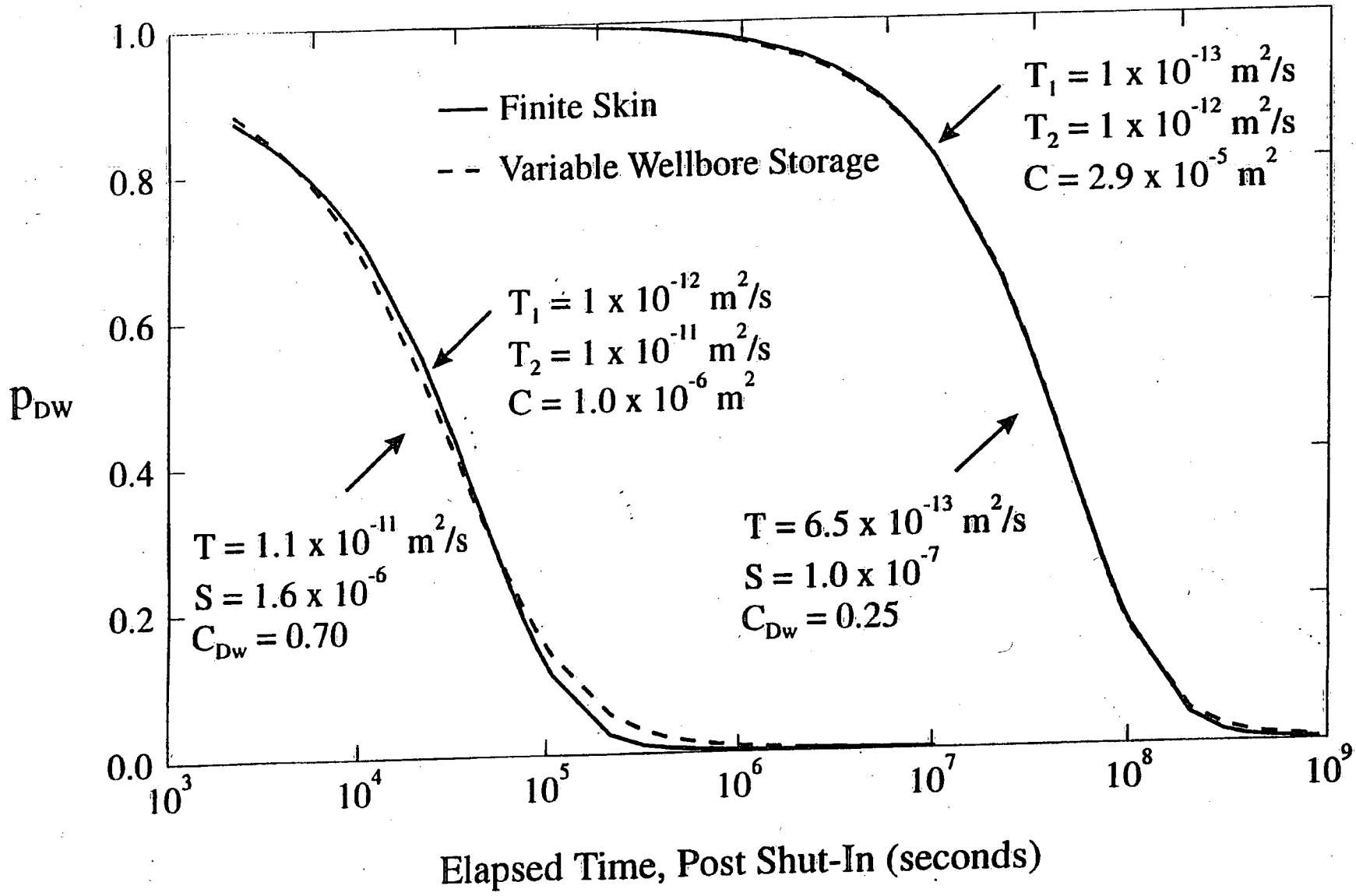

Figure 5 Comparison of the solutions for finite skin and variable wellbore storage for two different values of the wellbore storage factor, *C*.

Environment Canada | Environnement Canada

Canada

Canada Centre for Inland Waters
P.O. Box 5050
867 Lakeshore Road
Burlington, Ontario
L7R 4A6 Canada

National Hydrology Research Centre
11 Innovation Boulevard
Saskatoon, Saskatchewan
S7N 3H5 Canada

St. Lawrence Centre
105 McGill Street
Montreal, Quebec
H2Y 2E7 Canada

Place Vincent Massey
351 St. Joseph Boulevard
Gatineau, Quebec
K1A 0H3 Canada

Centre canadien des eaux intérieures
Case postale 5050
867, chemin Lakeshore
Burlington (Ontario)
L7R 4A6 Canada

Centre national de recherche en hydrologie
11, boul. Innovation
Saskatoon (Saskatchewan)
S7N 3H5 Canada

Centre Saint-Laurent
105, rue McGill
Montréal (Québec)
H2Y 2E7 Canada

Place Vincent-Massey
351 boul. St-Joseph
Gatineau (Québec)
K1A 0H3 Canada